

Effects of conformational isomerism on the desorption kinetics of *n*-alkanes from graphite

Kris R. Paserba and Andrew J. Gellman^{a)}

Department of Chemical Engineering, Carnegie Mellon University, Pittsburgh, Pennsylvania 15213

(Received 3 April 2001; accepted 11 July 2001)

The dynamics of oligomer desorption from surfaces have been studied by measuring the desorption kinetics of a set of *n*-alkanes from the surface of single crystalline graphite. Desorption rates were measured using a set of 21 monodispersed *n*-alkanes (C_NH_{2N+2} , $5 \leq N \leq 60$) each adsorbed at coverages in the range <0.1 to >1 monolayers. Desorption is observed to be a first-order process with a desorption barrier ($\Delta E_{\text{des}}^\ddagger$) that is independent of coverage. The pre-exponential of the desorption rate constant is independent of the oligomer chain length and has a value of $\nu = 10^{19.6 \pm 0.5} \text{ s}^{-1}$. We also find that $\Delta E_{\text{des}}^\ddagger$ has a nonlinear dependence on chain length and takes the empirical form $\Delta E_{\text{des}}^\ddagger = a + bN^\gamma$, with the exponent having a value of $\gamma = 0.50 \pm 0.01$. More interestingly, we have proposed a mechanism for the desorption process and a model for the energetics and the entropy of the oligomers on the surface that provide an extremely good quantitative fit to the observed chain length dependence of $\Delta E_{\text{des}}^\ddagger$. $\Delta E_{\text{des}}^\ddagger$ is given by the difference in energy between the gas phase *n*-alkane and the conformation of the adsorbed *n*-alkane with the minimum free energy at the desorption temperature. These results reveal that conformational isomerism plays a significant role in determining the desorption kinetics of oligomers from surfaces.

© 2001 American Institute of Physics. [DOI: 10.1063/1.1398574]

LIST OF SYMBOLS

$\Delta E_{\text{des}}^\ddagger$	desorption energy
N	chain length
a, b	constants in empirical fit
n	number of detached segments
r	rate of desorption
θ_n, θ	oligomer coverages
K_n	equilibrium constants for oligomer detachment
A_n	free energies of species with detached segments
k_{N-1}	rate constant for oligomer desorption
ΔE	energy to get last segment from surface
E^\ddagger	energy of desorption transition state
E_n	energy of species with n detached segments
q_\ddagger, q_n	partition functions
Γ	sum over equilibrium constants
S_n	entropy of species with n detached segments
α	intermolecular interaction parameter
γ	exponent in empirical fit

I. INTRODUCTION

The molecular structure and dynamics of macromolecular films adsorbed on surfaces are of fundamental importance to numerous technologies, including polymer flooding in enhanced oil recovery, lubricant coatings on magnetic storage disks, chromatographic separation, and protein adsorption on the surfaces of implants.¹ The study of polymers interacting with solid substrates is also of fundamental interest since these films represent examples of two-dimensional matter whose physical and chemical properties differ significantly

from those of their bulk phases.^{2–11} Theories describing the changes in material properties upon adsorption suggest that adsorption energies can be sufficient to overcome the loss of configurational entropy associated with adsorption and thus alter the conformation of the molecules from that observed in the bulk phase. The resulting structures of the adsorbed species typically show a high degree of orientational and positional order. In recent years much scientific research into the properties of adsorbed macromolecules has focused on understanding basic properties such as film thickness, coverage, and segment density distribution in the near-surface region.^{12–14} The results of these studies provide a comprehensive description of adsorbed polymer layers under equilibrium conditions.

In many situations adsorbed polymers and macromolecules do not reach an equilibrium state. The understanding of adsorbed polymers under conditions that are far from equilibrium is an important problem but one that has received considerably less attention than the study of equilibrium properties. For example, the kinetics of order–disorder transitions within adsorbed polymer films have a significant impact on phenomena such as polymer evaporation or desorption from surfaces. This is important in determining the rate of evaporative loss of lubricants from the surfaces of magnetic storage media, a process which generally leads to a substantial decrease in wear durability. The design of mechanical components for satellites requires knowledge of the rate of lubricant evaporation into the vacuum of space. As a final example the final step in the mechanism of Fischer–Tropsch synthesis of high molecular weight hydrocarbons is their desorption from the catalyst surface. All of these repre-

^{a)} Author to whom correspondence should be addressed.

sent examples of oligomer desorption processes from surfaces.

In this report we focus on understanding the kinetics and mechanism of the complex process by which oligomeric species desorb from surfaces. The dynamics of oligomer desorption from surfaces has been studied by measuring the desorption kinetics of *n*-alkanes (C_NH_{2N+2} , $N=5$ to 60) from the basal plane of single crystalline graphite into vacuum. Considerable progress has been made in the last 30 years in understanding *n*-alkane adsorption on graphite. Their adsorption isotherms from solution have been measured¹⁵ and the molecular structure of crystalline *n*-alkane monolayers adsorbed from solution at room temperature has been investigated using scanning tunneling microscopy (STM).^{16–21} These experiments suggest that over a considerable range of coverages *n*-alkanes adsorb in densely packed monolayers,^{15,22} with their carbon atoms in an all-*trans* conformation and their molecular backbone parallel to the surface. The *n*-alkanes that have been imaged have had chain lengths ranging from $C_{19}H_{40}$ to $C_{196}H_{386}$ and the observation of all-*trans* structures in each case indicates that the conformation at low temperatures is not dependent on molecular size. This suggests that the barrier to desorption, $\Delta E_{des}^\ddagger(N)$, might vary linearly with chain length, N . In this work we have shown that $\Delta E_{des}^\ddagger(N)$ for *n*-alkanes depends nonlinearly on N and demonstrate that this nonlinearity can be attributed to conformational disorder that occurs during heating.

The description of the desorption of a long flexible molecule from a surface must take into consideration the fact that the molecular structure has many degrees of freedom that provide many energetically equivalent trajectories leading to desorption. One such trajectory might be the simultaneous detachment of all segments from the surface. In this hypothetical process, $\Delta E_{des}^\ddagger(N)$ would be proportional to the number of monomers or chain length. There have been several previous studies which have investigated the effects of chain length on the desorption kinetics of alkyl alcohols and simple alkanes adsorbed on various surfaces. Zhang and Gellman used temperature programmed desorption (TPD) to study the reversible adsorption of a series of straight-chain alcohols [$CH_3(CH_2)_{N-1}OH$, $N=1$ to 5] on the Ag(110) surface and concluded that $\Delta E_{des}^\ddagger(N)$ increased incrementally by 4.6 ± 0.4 kJ/mole per methylene group in the hydrocarbon chain.²³ Millot *et al.* investigated the desorption of *n*-alkanes ($N=4$ to 8) from silicalite crystals using TPD and found that $\Delta E_{des}^\ddagger(N)$ also scaled linearly with chain length but in increments of 13.5 kJ/mole per methylene unit.²⁴ The desorption of *n*-alkanes ($N=6$ to 12) from the Au(111) surface was studied by Wetterer *et al.* using helium atom reflectivity.²⁵ Their conclusions from this study indicate that $\Delta E_{des}^\ddagger(N)$ increased incrementally by 6.2 ± 0.2 kJ/mole per methylene unit. In these cases the range of alkyl chain lengths has been limited to $N \leq 12$. Needless to say, it is not surprising that over this limited range $\Delta E_{des}^\ddagger(N)$ would appear to be linear in chain length.

The conclusions drawn from the previous studies of oligomer desorption are limited by the limited range of the alkyl chain lengths. By nature, longer chain molecules possess more degrees of freedom and therefore more possible

conformations when adsorbed on a surface. Any deviation from the all-*trans* structures observed in the room temperature STM images of *n*-alkanes would tend to cause a decrease in ΔE_{des}^\ddagger as a result of the displacement of the methylene groups away from the surface. In other words, if long chain oligomers adopt less ordered structures on a surface, $\Delta E_{des}^\ddagger(N)$ would not scale linearly with chain length. Such disorder has been observed in variable temperature STM images of long chain *n*-alkanes adsorbed on graphite which indicate that a multitude of conformations may be adopted at elevated surface temperatures. Askadskaya and Rabe²⁶ used a variable temperature STM to image monolayer coverages of $C_{24}H_{50}$ and $C_{32}H_{66}$ on graphite in air. High-resolution images of each monolayer were obtained at 297, 303, 313, and 318 K. At 297 K, highly ordered lamellae of the *n*-alkanes were observed with their carbon atoms in an all-*trans* conformation and their molecular backbone parallel to the surface. Heating to 303 K induced a small dynamic roughening of the lamellae. Further heating to 313 K caused a continuing increase in roughness, however, the spacing between the molecules within the lamella remained essentially constant. Finally at 318 K no molecular structure was observed for the *n*-alkanes on graphite. Upon cooling, the lamellae assumed their original structures, indicating the reversible nature of the disordering observed with the STM. The fundamentally important result of that work is that substrate temperature will affect the conformations of adsorbed oligomers by causing deviations from the all-*trans* configurations observed at low temperature.^{16–21}

Thermally induced disorder and conformational defects in *n*-alkane monolayers on graphite have also been investigated by Bucher *et al.*²⁷ STM images were recorded for $C_{28}H_{58}$ and $C_{32}H_{66}$ at 281 and 300 K, respectively. At 281 K the monolayers of each molecule formed lamellar structures with the molecules in an all-*trans* conformation, as previously reported. In an effort to investigate the thermal disordering of these monolayers, Bucher *et al.* utilized a quench technique whereby the graphite substrate was heated to a temperature near the bulk melting point of the adsorbed *n*-alkane and then rapidly cooled at a rate of 200 K/min to a final temperature of 283 K. This rapid quenching allowed “frozen-in” structures of the high temperature phase to be imaged using the STM. During these experiments, the monolayers of $C_{28}H_{58}$ and $C_{32}H_{66}$ on the graphite surface were heated to 346 and 342 K, respectively. The choice of temperatures was made so as to allow study of the conformational disorder that occurs at temperatures both slightly below ($C_{32}H_{66}$) and slightly above ($C_{28}H_{58}$) the bulk melting points of the *n*-alkanes. After quenching, STM images were recorded for $C_{28}H_{58}$ and $C_{32}H_{66}$ at 279 and 287 K, respectively. In each case, the STM images revealed a significant loss of molecular order. The identity of the individual lamellae present in the low temperature equilibrium structure was completely lost in the quenched films as a result of conformational disorder. These phenomena are similar to those observed by Askadskaya and Rabe in their studies.²⁶ All the variable temperature STM images of long chain *n*-alkanes adsorbed on graphite suggest that heating causes displacement of methylene groups from the surface and might

thereby decrease $\Delta E_{\text{des}}^{\ddagger}$ relative to that expected for *n*-alkanes in an all-*trans* conformation.

Molecular dynamics (MD) simulations have also proved to be a valuable method for investigating the conformation of adsorbed molecules. Hansen *et al.*²⁸ reported MD simulations of the melting behavior of $\text{C}_{32}\text{H}_{66}$ adsorbed on graphite. Both the intermolecular and intramolecular potential energies per $\text{C}_{32}\text{H}_{66}$ molecule were calculated as a function of temperature and simultaneously exhibited an inflection point at ~ 350 K. This behavior was attributed to the onset of both intermolecular and intramolecular disorder at the melting point of the $\text{C}_{32}\text{H}_{66}$ monolayer. To further support this assertion, the probability that each of the 29 dihedral bonds present in a $\text{C}_{32}\text{H}_{66}$ molecule was in a gauche conformation was calculated at five temperatures ranging from 250 to 500 K. In general the distributions displayed a similar form at all temperatures and were characterized by a constant level of gauche defects in the middle of the molecule with a higher number of defects at the chain ends. More importantly, the probability of an internal bond being in a gauche conformation increased from less than 1% at 250 K (indicating an all-*trans* structure) to nearly 40% at 500 K. The probabilities also increased dramatically in the temperature range 325–375 K, a finding that is consistent with the inflection point of 350 K observed in the intermolecular and intramolecular potential energies of $\text{C}_{32}\text{H}_{66}$. As with the studies mentioned above, this work provides conclusive evidence that substrate temperature is expected to alter the conformation of adsorbed molecules and thereby change $\Delta E_{\text{des}}^{\ddagger}$.

The detachment of a polymer chain from a surface has also been investigated theoretically by Haupt *et al.*²⁹ Their studies involved predicting force-extension profiles measured using an atomic force microscopy (AFM) tip to pull an isolated polymer molecule from a weakly adsorbing surface under differing rates of extension. The model used consisted of an ideal or Gaussian chain of monomers some fraction of which adsorb on a surface with a characteristic adsorption energy of εRT . Each of these contacts separates the polymer into a series of loops and tails. The AFM tip is allowed to contact a loop or tail and extend it some distance orthogonal to the surface while simultaneously measuring the force needed for this process. In order to detach a chain from the surface, all of the monomers contacting the surface must be released. At fast extension rates, the theoretical force profile (i.e., force versus extension distance) resembles a sawtooth structure with the discontinuities resulting from the detachment of individual contact points separating the pulled loop from an adjacent loop. The maximum force at each sawtooth represents the detachment force, which decreases with loss of successive monomers. These trends have also been observed in AFM experiments and clearly illustrate that the detachment of the adsorbed monomer trains does not occur simultaneously but instead follows a sequential mechanism. On the basis of these findings it is reasonable to suggest that the desorption of polymer molecules from surfaces has a $\Delta E_{\text{des}}^{\ddagger}$ that does not scale linearly with chain length.

Quantitative studies have recently been reported in which the desorption or detachment of homopolymer chains from a solid surface has been suggested to have a $\Delta E_{\text{des}}^{\ddagger}$ that

scales nonlinearly with chain length. Wang *et al.* used dynamic Monte Carlo simulations to model the desorption of homopolymer chains having lengths of $N=5$ to 85.³⁰ Their model of the system was framed in terms of polymer configurations consisting of trains of segments in contact with the surface, separated by loops of detached segments, and terminated by tails which are also detached from the surface. Their conclusions were that the average lifetime, τ , of an adsorbed polymer chain on the surface can be described by a power law ($\tau \propto N^\gamma$); where the exponent has a value of $\gamma = 2.5 \pm 0.1$. More importantly, the average train length, N_{tr} , and the average number of trains in a chain, n_{tr} , were calculated under the conditions of the simulations and revealed that N_{tr} reaches an asymptotic limit of 10 segments for large N . In this limiting case, $\Delta E_{\text{des}}^{\ddagger}$ for chain detachment would no longer increase in proportion to N .

Although the studies detailed above have been informative, a mechanistic and quantitative study of the effect of chain length on polymer desorption is still needed. This study represents the first set of measurements of desorption kinetics to use a broad enough range of oligomer chain lengths to allow a quantitative description of the nonlinear dependence of $\Delta E_{\text{des}}^{\ddagger}$ on chain length. Desorption rates from graphite were measured using temperature programmed desorption (TPD) for a series of 21 *n*-alkanes ranging in length from C_5H_{12} to $\text{C}_{60}\text{H}_{122}$. Desorption is observed to be a first-order process with a $\Delta E_{\text{des}}^{\ddagger}$ that is roughly independent of coverage. The pre-exponent of the desorption rate constant was measured to be $\nu = 10^{19.6 \pm 0.5} \text{ s}^{-1}$ and is independent of the *n*-alkane oligomer chain length, N . The desorption energy does not scale linearly with chain length and takes the empirical form $\Delta E_{\text{des}}^{\ddagger} = a + bN^\gamma$ with the exponent having a value of $\gamma = 0.50 \pm 0.01$. More interestingly we have been able to propose a mechanism for the desorption process and a model for the energy and the entropy of the oligomers on the surface that provides an extremely good quantitative fit to the observed chain length dependence of $\Delta E_{\text{des}}^{\ddagger}$. These results reveal that conformational entropy plays a significant role in determining the desorption kinetics of oligomers from surfaces.

II. EXPERIMENT

All experiments were conducted in a stainless steel ultrahigh vacuum (UHV) chamber with a base pressure of 10^{-9} Torr achieved through use of an ion-pump and titanium sublimation pump. TPD experiments were performed using an ABB Extrel Merlin quadrupole mass spectrometer (QMS). This instrument has a mass range of 1–500 amu and is capable of simultaneously monitoring up to five masses as a function of time during a TPD experiment.

The substrate used was a $12 \times 12 \times 2$ mm piece of highly oriented pyrolytic graphite (HOPG). Prior to mounting, the sample was cleaved in air to expose the basal plane. The graphite was then mounted on a square piece of tantalum foil ~ 0.25 mm thick using electrically conductive silver epoxy (Aremco Co.). Two tantalum wires were spotwelded to the rear of the tantalum foil and mounted to the end of a manipulator capable of *x*, *y*, and *z* translation and 360 °C rota-

tion. Once mounted the graphite could be cooled to ~ 120 K through mechanical contact with a liquid nitrogen reservoir at the end of the manipulator. In addition, the graphite substrate could be heated resistively at a constant rate using a computer to provide proportional-derivative temperature control. The temperature of the tantalum foil was measured using a chromel-alumel thermocouple spotwelded to its rear face. The temperature of the graphite sample was assumed to be that of its tantalum foil mount.

Prior to each set of TPD experiments conducted with a given n -alkane, the graphite sample was heated in vacuum to ~ 1200 K to induce the desorption of any adsorbed contaminants. Surface cleanliness of the graphite sample has been assumed based on observations made in previous studies.^{31,32} In addition, desorption spectra were highly reproducible, indicating that no contamination of the surface occurred due to adsorbate decomposition. The desorption peaks for submonolayer coverages of heptane (C_7H_{16}) were used to assess the reproducible nature of the spectra. During a normal TPD experiment using heptane the desorption temperature was consistently found to be 211 K and the width of the desorption peak was <7 K.

A set of n -alkanes (C_NH_{2N+2} , $N=5, 6, 7, 8, 10, 12, 14, 16, 18, 20, 22, 24, 26, 44, 60$) were purchased having purities of $>98\%$ from Aldrich Chemicals. Acros Chemicals supplied n -alkanes ($N=28, 32, 36, 40$) in purities of $>97\%$. Fluka Chemicals provided n -alkanes ($N=48, 56$) with purities of $>97\%$. All compounds purchased in liquid form were purified through a series of freeze-pump-thaw cycles designed to remove any high vapor pressure contaminants. Compounds purchased in solid form were purified by heating the sample in a glass vial under vacuum for ~ 12 h at temperatures ranging from 60 (for $C_{18}H_{38}$) to 280°C (for $C_{60}H_{122}$). The purity of the compounds was further verified by measuring the heats of vaporization directly from multilayer desorption peaks generated in their TPD spectra and comparing these results with values reported in the literature. These data will be presented in later sections of this report.

Exposure of the graphite surface to the n -alkanes with carbon number $N \leq 12$ was performed using leak valves fitted with stainless steel dosing tubes to introduce alkane vapor into the UHV chamber. Introducing vapor of the n -alkanes with $N > 12$ required alternate methods. One of the features of the higher molecular weight n -alkanes that prevents introduction of their vapor into the UHV chamber through a leak valve is that they exhibit very low vapor pressures even at high temperatures. Vapor pressures of the n -alkanes with $N > 26$ are expected to be on the order of 10^{-9} Torr or less at 100°C .^{33,34} This was the reason for the construction of the high mass deposition source shown in Fig. 1. The n -alkane to be used as an adsorbate is housed in a glass vial and coupled to a stainless-steel tube enclosed in a linear translation unit. The entire deposition source is under vacuum and isolated from the main UHV chamber by a gate valve. A heating jacket (Glascol Co.) with a maximum temperature of 450°C is used to heat the bulk adsorbate to the temperature necessary to induce its vaporization. During dosing the linear translation unit allows the stainless steel tube to be extended

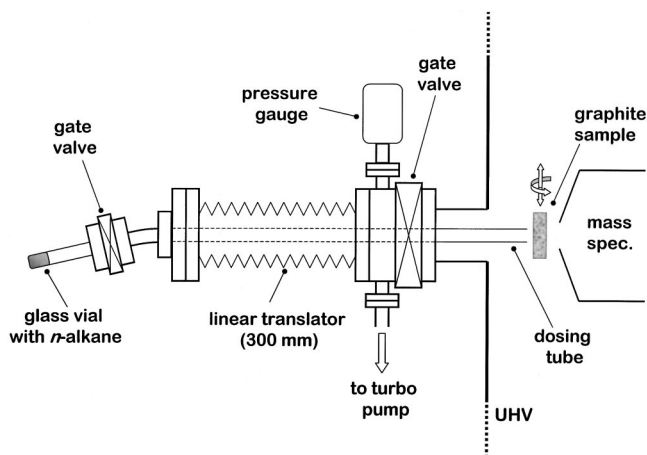


FIG. 1. Schematic illustration of the high mass deposition source used in this work. The n -alkane to be deposited onto the graphite substrate is housed in a glass vial at the end of a linear translator. A dosing tube extends the length of the linear translator and may be extended into the UHV chamber during deposition. The n -alkane is vaporized in the glass vial using a heating jacket and the vapor travels the length of the dosing tube to be adsorbed onto the graphite substrate.

into the UHV chamber and positioned directly in front of the substrate. The vapor of the adsorbate travels from the glass vial down the length of the stainless steel tube and is deposited onto the substrate which is held at ~ 120 K.

Within the UHV chamber the graphite substrate was positioned to face either the stainless steel dosing tubes from the leak valves or the stainless steel dosing tube from the high mass deposition source. TPD studies were performed by cooling the graphite sample in UHV to ~ 120 K and exposing its surface to vapor of the n -alkanes. Following adsorption of the n -alkanes on the graphite surface, the substrate was positioned approximately 2 cm from an aperture leading to the QMS and heated at a constant rate to the temperatures necessary to induce the desorption of all adsorbed species. During heating, the QMS was used to monitor the desorption rate of the adsorbed n -alkanes and any decomposition products if present. In all cases, adsorption of the n -alkanes was both molecular and reversible with no indication of decomposition.

III. RESULTS

The rate of a first-order desorption process from a surface is expressed as

$$r = -\frac{d\theta}{dt} = k\theta = \nu \cdot \exp\left(-\frac{\Delta E_{\text{des}}^\ddagger}{RT}\right)\theta, \quad (1)$$

where r is the desorption rate, θ is the fractional surface coverage of the adsorbed species, k is the desorption rate constant, ν is a pre-exponential factor for desorption, $\Delta E_{\text{des}}^\ddagger$ is the desorption barrier, R is the universal gas constant, and T is temperature. The following sections describe the determination of the values of ν and $\Delta E_{\text{des}}^\ddagger$ for n -alkanes in the length range C_5H_{12} through $C_{60}H_{122}$ adsorbed on graphite.

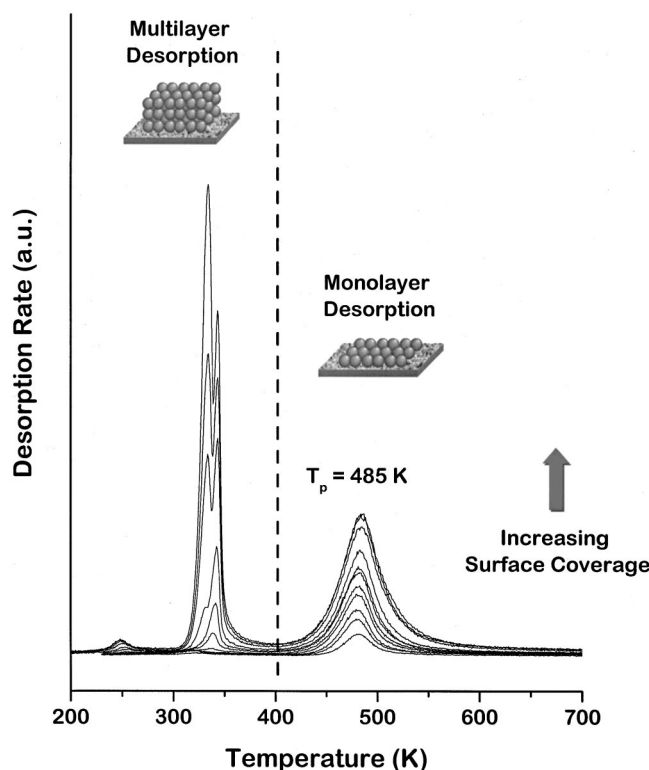


FIG. 2. TPD spectra of $C_{28}H_{58}$ adsorbed at various coverages on the graphite surface at 120 K. The desorption peak centered at 485 K is assigned to desorption of the $C_{28}H_{58}$ monolayer. The desorption features at 334 and 344 K are assigned to desorption of $C_{28}H_{58}$ multilayers. The monolayer desorption temperature is independent of coverage and indicates a first-order desorption process with a coverage-independent $\Delta E_{des}^{\ddagger}$. The spectra were generated using a mass spectrometer to monitor the signal at $m/q = 57$ ($C_4H_9^+$). The heating rate was 2 K/s.

A. Evaluation of reaction order for *n*-alkane desorption from graphite

Prior to any detailed analysis of the kinetics of alkane desorption it is necessary to ascertain that the desorption process is indeed first-order and describable by Eq. (1). The order of the desorption reaction and $\Delta E_{des}^{\ddagger}$ of the *n*-alkanes on graphite have been measured by performing TPD experiments using a constant heating rate, β , of 2 K/s and initial *n*-alkane coverages ranging from submonolayers to many multilayers. Figure 2 shows the TPD spectra of $C_{28}H_{58}$ for different coverages initially adsorbed on the graphite surface at 120 K. Deposition of $C_{28}H_{58}$ was performed by heating the bulk phase to 110 °C in the high molecular weight doser. No decomposition of $C_{28}H_{58}$ is expected at this temperature based on reports indicating a bulk decomposition temperature of 400 °C for the *n*-alkanes.^{35,36} The TPD spectra were generated by using the QMS to monitor the signal at $m/q = 57$ ($C_4H_9^+$) during heating. Several additional mass-to-charge ratios were monitored including $m/q = 71$ ($C_5H_{11}^+$), $m/q = 85$ ($C_6H_{13}^+$), and $m/q = 99$ ($C_7H_{15}^+$) to detect the desorption of any decomposition products if present. The desorption signals at these m/q ratios all occurred at the same temperatures suggesting that they are all due to desorption of the same molecule and that there is no decomposition of the

$C_{28}H_{58}$ on graphite during heating. No decomposition of any of the *n*-alkanes studied was observed on the graphite surface during heating.

At the lowest coverage, $C_{28}H_{58}$ desorbs over a relatively narrow temperature range and achieves a maximum rate of desorption at 481 K as shown in Fig. 2. As the *n*-alkane exposure to the surface is increased, the desorption peak increases in intensity and shifts to slightly higher temperatures. At highest coverage the $C_{28}H_{58}$ monolayer desorbs at 485 K. As the *n*-alkane exposure is further increased a second desorption feature grows in at ~ 344 K which indicates the onset of multilayer desorption. This low temperature desorption feature continues to grow with increasing coverage and displays zero-order kinetics. Upon further *n*-alkane exposure to the graphite surface, a third desorption feature grows in at ~ 334 K that also is characteristic of multilayer desorption. This double peak structure observed in the multilayer desorption of $C_{28}H_{58}$ is consistently observed for all the longer chain *n*-alkanes. Although its origin is not known it is possible that this is due to desorption from the second and then the third *n*-alkane layers on the graphite surface.

The heat of vaporization, ΔH_{vap} , has been used in this study as a basis for establishing the effectiveness of the techniques used to purify the alkanes. The value of ΔH_{vap} for $C_{28}H_{58}$ has been determined using the relation

$$\frac{d \ln r}{d(1/T)} = - \frac{\Delta E_{des}^{mult}}{R} \quad (2)$$

to measure the desorption energy for the multilayer, ΔE_{des}^{mult} , by using the leading edge of the multilayer desorption peak which exhibits zero-order desorption kinetics. ΔE_{des}^{mult} should be close to the heat of bulk vaporization, ΔH_{vap} , of $C_{28}H_{58}$. The data for the desorption of the $C_{28}H_{58}$ multilayer are presented in Fig. 3 and reveal that ΔE_{des}^{mult} of $C_{28}H_{58}$ is 153.8 ± 1.5 kJ/mole. This is consistent with the ΔH_{vap} of $C_{28}H_{58}$ reported in the literature using various experimental techniques. Piacente *et al.* conducted both Knudsen effusion and torsion effusion studies on $C_{28}H_{58}$ and determined the ΔH_{vap} to be 156.6 ± 27.7 kJ/mole and 151.2 ± 3.8 kJ/mole from each measurement, respectively.³⁷ Transpiration studies of $C_{28}H_{58}$ conducted by Grenier-Loustalot *et al.* indicated a heat of vaporization of roughly 157.6 ± 9.4 kJ/mole.³⁸ Chirico *et al.* found the ΔH_{vap} for $C_{28}H_{58}$ to be 150.7 ± 2.9 kJ/mole using inclined piston measurements.³⁹ The agreement between ΔE_{des}^{mult} for $C_{28}H_{58}$ in this work and the values of ΔH_{vap} reported in the literature indicates that the purified $C_{28}H_{58}$ sample is free of any low mass contaminants (such as short-chain *n*-alkanes possibly used in their synthesis). Using a similar procedure, the ΔH_{vap} of each *n*-alkane used was evaluated and compared with values reported in the literature. Table I summarizes the multilayer desorption temperatures observed for the *n*-alkanes with $N \leq 32$ as well as ΔE_{des}^{mult} determined in this study and the ΔH_{vap} reported in the literature. Values of ΔE_{des}^{mult} for the *n*-alkanes with $N > 32$ were not determined since the exposures needed to generate the multilayer films on the graphite surface were too high.

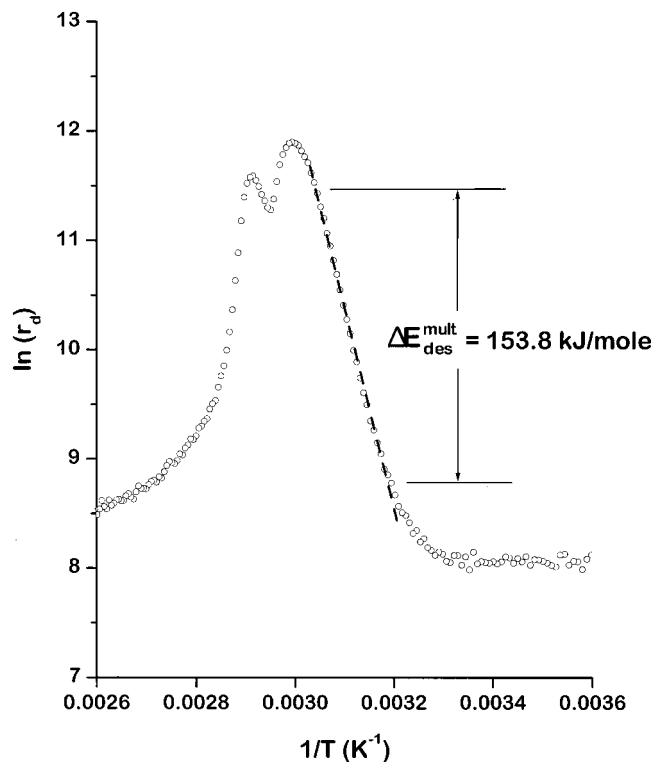


FIG. 3. Arrhenius representation of the TPD spectrum for $C_{28}H_{58}$ measured at highest coverage. A line has been fit to the leading edge of the multilayer desorption feature and measures the ΔE_{des}^{mult} for $C_{28}H_{58}$ to be 153.8 ± 1.5 kJ/mole.

The dependence of the desorption spectra on n -alkane coverage is similar for all of the n -alkanes studied. In general terms both the monolayer and multilayer peak desorption temperatures, T_p , increase with chain length, N . In all cases the desorption temperature of the monolayer is nearly independent of the n -alkane coverage indicating that the desorption process is first-order and that there is little coverage dependence to the desorption barrier, ΔE_{des}^\ddagger . The change in T_p in the submonolayer regime varied from a minimum of 0.5 K for $C_{60}H_{122}$ to a maximum of 7 K for C_5H_{12} . The small change in the T_p of the n -alkanes at these coverages indicates that there is very little coverage dependent interaction between the adsorbed molecules. Attractive interactions are observed for the n -alkanes with $N < 16$ but are not significant enough to justify an analysis other than the use of a simple first-order rate expression. This is consistent with the analysis of n -alkane ($N = 5$ to 10) desorption from metal surfaces such as Cu(100).^{40–43} The dependence of peak shape and peak position on factors such as coverage of the n -alkanes resembled that of a simple first-order desorption process in both studies on Cu(100). The T_p increased by ~ 4 K when increasing the coverage from 25 to 100% of a monolayer.⁴² This result indicates that little interaction occurs between the n -alkane molecules. The interactions that were observed are attractive and at monolayer saturation their magnitude was roughly 2% that of ΔE_{des}^\ddagger on the Cu(100) surface. On the basis of these studies and the observations made thus far in the current work it is reasonable to suggest that the n -alkanes

TABLE I. Multilayer peak desorption temperatures for the n -alkanes and their corresponding desorption energies, ΔE_{des}^{mult} . Two multilayer desorption features (α and β peaks) are observed for the n -alkanes with $N \geq 18$ and their desorption temperatures are reported as T_p^α and T_p^β . The purity of the n -alkanes has been ascertained by comparing the measured values of ΔE_{des}^{mult} with the ΔH_{vap} reported in the literature. NA=not applicable ND=not determined.

Chain length, N	T_p^α (K)	T_p^β (K)	Measured ΔE_{des}^{mult} (kJ/mole)	ΔH_{vap} (kJ/mole)
5	133	NA	24.2 ± 3.3	26.4 (Ref. 40)
6	143	NA	31.2 ± 0.2	31.5 (Ref. 40)
7	154	NA	38.2 ± 0.4	36.6 (Ref. 40)
8	171	NA	46.2 ± 0.2	41.6 (Ref. 40)
10	193	NA	52.4 ± 0.2	51.4 (Ref. 40)
12	224	NA	59.0 ± 0.7	61.5 (Ref. 40)
14	239	NA	70.3 ± 0.6	71.7 (Ref. 40)
16	258	NA	74.8 ± 0.5	81.4 (Ref. 40)
18	273	278	90.4 ± 0.6	91.4 (Ref. 40)
20	288	294	108.1 ± 1.5	101.8 (Ref. 40)
22	298	307	118.3 ± 2.5	120.1 (Ref. 37)
24	315	321	132.2 ± 1.5	134.8 (Ref. 37)
26	322	332	128.9 ± 3.3	146.1 (Ref. 37)
28	334	344	153.8 ± 1.5	151.2 (Ref. 37)
32	353	363	182.9 ± 1.9	190.1 (Ref. 41)
36	370	382	ND	212.6 (Ref. 41)
40	388	399	ND	235.1 (Ref. 41)
44	413	ND	ND	257.6 (Ref. 41)
48	430	ND	ND	280.2 (Ref. 41)
56	456	ND	ND	325.2 (Ref. 41)
60	467	ND	ND	347.7 (Ref. 41)

desorb from the graphite surface with first-order, coverage independent kinetics.

B. Measurement of ΔE_{des}^\ddagger and ν for n -alkanes from graphite

TPD experiments performed with a constant heating rate and variable coverages of n -alkanes on graphite have shown that the desorption kinetics of this system may be represented by a simple first-order expression. As a first approximation, the pre-exponential factor, ν , shown in Eq. (1) generally assumes a value of 10^{13} s^{-1} based on conventional transition state theory.⁴⁴ However, past studies indicate that this approximation is not always valid for first-order desorption processes.^{45–47} These data suggest that an experimental determination of the pre-exponential factors is required for the accurate analysis of the kinetics governing the desorption of molecules from surfaces. We present below two methods used to determine both ν and ΔE_{des}^\ddagger from the TPD spectra. Section III B 1 describes the analysis of desorption data using a simple Redhead method,⁴⁸ while Sec. III B 2 focuses on obtaining the kinetic parameters through fitting of the TPD spectra to simulated spectra obtained by numerical integration of the desorption equation.

1. Desorption kinetic parameters determined by Redhead analysis

With the details above in mind we have measured both ν and ΔE_{des}^\ddagger independently for a subset of nine n -alkanes ($C_N H_{2N+2}$, $N = 7, 12, 24, 26, 28, 36, 40,$ and 44) in an effort to accurately interpret their desorption kinetics from graph-

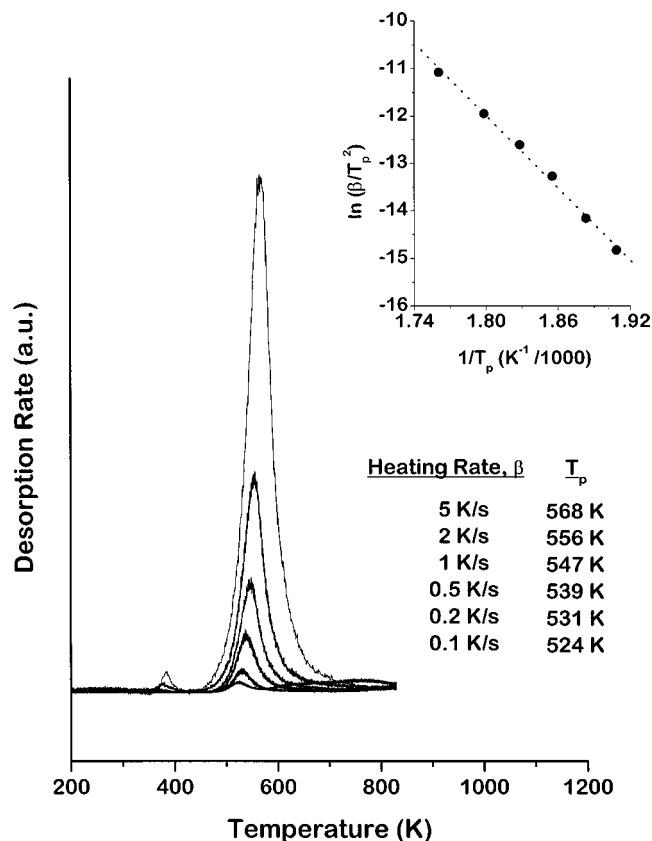


FIG. 4. TPD spectra of $C_{36}H_{74}$ measured at varying heating rates (β) for initial coverages of approximately one monolayer. Heating rates varying from 0.1 to 5 K/s were used to desorb the $C_{36}H_{74}$ monolayer. The monolayer desorption temperatures increase with increasing heating rate. The spectra were generated using a mass spectrometer to monitor the signal at $m/q = 57$ ($C_4H_9^+$) during heating. The inset is a plot of $\ln(\beta/T_p^2)$ vs $1/T_p$ for the desorption of $C_{36}H_{74}$ from the graphite surface. The slope of the linear fit has been used to estimate the ΔE_{des}^\ddagger for $C_{36}H_{74}$ from graphite.

ite. TPD spectra were recorded for the *n*-alkanes at various heating rates, β , using initial coverages of approximately one monolayer. The heating rates used in each set of experiments varied from 0.1 K/s to 5 K/s. Figure 4 illustrates the variable heating rate TPD spectra for $C_{36}H_{74}$ generated by using the QMS to monitor the signal at $m/q = 57$ ($C_4H_9^+$). The $C_{36}H_{74}$ monolayer desorbs with a maximum rate from the graphite surface at $T_p = 524$ K when the substrate was heated at 0.1 K/s. As the heating rate was increased in subsequent experiments, the desorption peaks intensified and shifted to higher temperatures. TPD experiments using a heating rate of 5 K/s induced desorption of the $C_{36}H_{74}$ monolayer at $T_p = 568$ K.

Analysis of the heating rate dependence of the peak desorption temperature can be used to determine ν and ΔE_{des}^\ddagger independently. TPD data presented in the form $\ln(\beta/T_p^2)$ versus $1/T_p$ should yield a line with a slope equal to $-\Delta E_{des}^\ddagger/R$.⁴⁸ Shown in the inset to Fig. 4 is a plot of $\ln(\beta/T_p^2)$ versus $1/T_p$, where T_p is dependent on the heating rate, β . A linear regression performed on the data in the inset of Fig. 4 indicates that $\Delta E_{des}^\ddagger = 211.5 \pm 6.9$ kJ/mole for $C_{36}H_{74}$. Figure 4 and its inset qualitatively illustrate the desorption behavior for all the *n*-alkanes studied using variable heating rate TPD experiments. Values of ν and ΔE_{des}^\ddagger for the other *n*-alkanes studied using variable heating rate TPD ex-

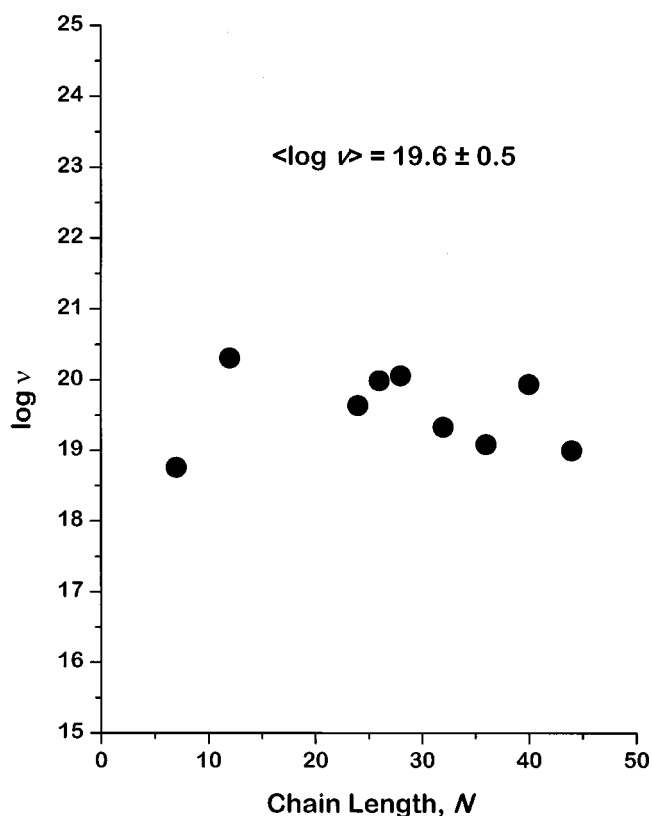


FIG. 5. Pre-exponential factors, ν , of the first-order desorption rate constants, k , for the *n*-alkanes of varying chain length ($N=7$ to 44). The values of ν were calculated using a Redhead analysis from the TPD spectra measured at varying heating rates ($\beta=0.1$ to 5 K/s). The pre-exponential factors range from 10^{19} to 10^{20} s⁻¹ and are significantly greater than $k_B T/h \approx 10^{13}$ s⁻¹. The value of $\log(\nu)$ is nearly independent of chain length.

periments were calculated in a similar manner to that outlined above.

With ΔE_{des}^\ddagger of the *n*-alkanes measured, it is possible to evaluate the pre-exponential factors for desorption for each *n*-alkane studied using variable heating rate TPD experiments. The pre-exponential factors for desorption, ν , may be estimated using Redhead's equation⁴⁸ for first-order kinetics

$$\nu = \frac{\beta \Delta E_{des}^\ddagger}{RT_p^2} \exp\left(\frac{\Delta E_{des}^\ddagger}{RT_p}\right), \quad (3)$$

where T_p depends on the heating rate β . As indicated by Eq. (3), a pre-exponential factor for desorption may be calculated at each heating rate. Figure 5 illustrates the averaged pre-exponential factors as a function of chain length, N , for each *n*-alkane studied using variable heating TPD experiments. Note that the y-axis is displayed in the form of $\log(\nu)$. The fundamentally important result is that the pre-exponential factors for desorption of *n*-alkanes from graphite assume values in the range 10^{19} – 10^{20} s⁻¹, as opposed to the value of 10^{13} s⁻¹ that is commonly assumed in analysis of TPD spectra. In addition, the value of ν is roughly independent of the chain length with an average value of $\nu_{avg} = 10^{19.6 \pm 0.5}$ s⁻¹. The values of both ν and ΔE_{des}^\ddagger for the *n*-alkanes studied using variable heating rate TPD experiments will be compared with values obtained by fitting to simulated TPD spectra as outlined below in the next section.

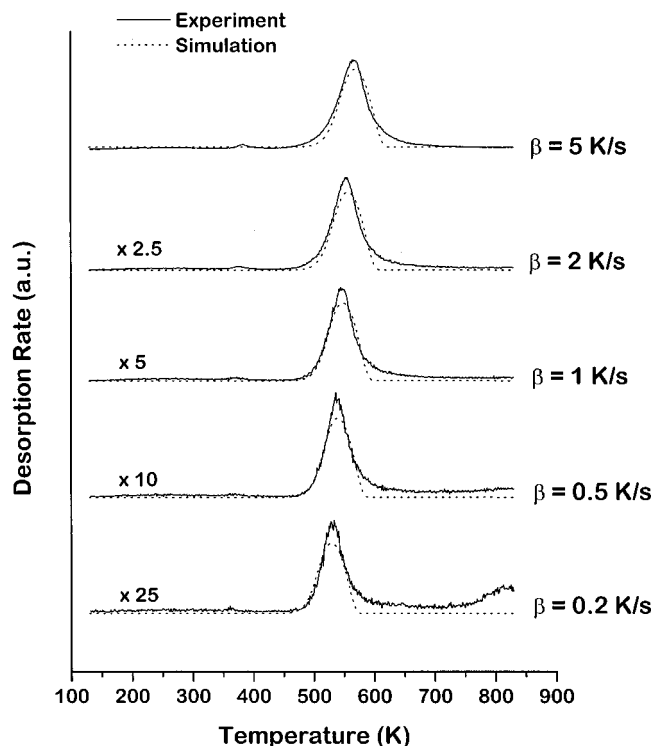


FIG. 6. Fits of simulated desorption spectra to the TPD spectra recorded for $C_{36}H_{74}$ at varying heating rates ($\beta=0.2$ to 5 K/s). The solid lines represent the measured TPD spectra while the dashed lines indicate the simulated spectra. The free parameters used in the minimization were found to have values of $\Delta E_{des}^{\ddagger}=215.3$ kJ/mole, $\nu=10^{18.7}$ s $^{-1}$, and $\alpha=0.052$. Both $\Delta E_{des}^{\ddagger}$ and ν are of the same magnitude as those calculated using a Redhead analysis of the TPD data.

2. Desorption kinetic parameters determined by simulation

In addition to using the Redhead analysis, a second approach was used to obtain values for the pre-exponential factors, ν , and the desorption barriers, $\Delta E_{des}^{\ddagger}$, of the nine n -alkanes studied using variable heating rate TPD experiments. This approach involved fitting the TPD spectra to spectra simulated using the following expression for the desorption rate:

$$r = \nu \cdot \exp\left(-\frac{\Delta E_{des}^{\ddagger}(1 - \alpha\theta)}{RT}\right) \theta. \quad (4)$$

The variable α is an intermolecular interaction parameter. The value of α is positive for repulsive interactions and negative for attractive interactions. A modified version of Powell's method for minimization was used to fit spectra generated by integrating Eq. (4) with the experimental TPD spectra. This fitting procedure used ν , $\Delta E_{des}^{\ddagger}$, and α as free parameters that were allowed to vary to optimize the fit. The TPD spectra recorded at all heating rates for an n -alkane were fit simultaneously to determine the best values of ν , $\Delta E_{des}^{\ddagger}$, and α for each molecule. The TPD spectra of $C_{36}H_{74}$ and the simulated spectra obtained from Eq. (4) are shown in Fig. 6 for heating rates of $\beta=0.2$ – 5 K/s and are indicative of the fits obtained for the TPD spectra of the remaining eight n -alkanes analyzed in this manner. The free parameters for $C_{36}H_{74}$ assumed final values of $\nu=10^{18.7}$ s $^{-1}$, $\Delta E_{des}^{\ddagger}$

TABLE II. Desorption barriers, $\Delta E_{des}^{\ddagger}$, and the pre-exponential factors, ν , of the n -alkanes determined from both a Redhead analysis and by simulation variable heating rate TPD data.

Chain length, N	$\log(\nu)^a$	$\log(\nu)^b$	$\Delta E_{des}^{\ddagger}$ (kJ/mole) ^a	$\Delta E_{des}^{\ddagger}$ (kJ/mole) ^b
7	18.7 ± 0.3	18.8	76.4 ± 1.0	76.4
12	20.3 ± 0.3	19.1	116.6 ± 1.5	109.9
24	19.6 ± 0.8	19.3	171.3 ± 6.3	175.4
26	19.0 ± 0.6	18.4	174.3 ± 5.0	170.4
28	20.1 ± 0.3	18.8	191.2 ± 3.0	182.9
32	19.3 ± 0.8	18.7	200.1 ± 8.2	200.4
36	19.1 ± 0.7	18.7	211.5 ± 6.9	215.3
40	19.9 ± 0.7	19.3	233.8 ± 7.8	237.8
44	19.0 ± 0.6	20.3	235.9 ± 6.8	266.9

^aCalculated using a Redhead analysis of variable heating rate TPD data.

^bCalculated through a least squares minimization of the variable heating rate TPD data.

= 215.3 kJ/mole, and $\alpha=0.052$. For comparison, the values of ν and $\Delta E_{des}^{\ddagger}$ determined from both the simulation and the Redhead methods are given in Table II for all nine n -alkanes studied using variable heating rate TPD. The data presented in Table II illustrate that the pre-exponential factors determined through fitting assume values that are approximately 10^{19} – 10^{20} s $^{-1}$ and are independent of the chain length. The average pre-exponential factor calculated through fitting was found to be $\nu_{avg}=10^{19.1 \pm 0.6}$ s $^{-1}$ and is similar in magnitude to the value ($\nu_{avg}=10^{19.6 \pm 0.5}$ s $^{-1}$) found through the Redhead analysis.

The significant conclusion from the data presented in Table II is that a single averaged pre-exponential factor may be used with confidence to model the desorption kinetics for *all* of the n -alkanes studied. The fact that the desorption pre-exponent is independent of chain length, N , suggests that its high value is due to a degree of freedom common to all of the n -alkanes such as center of mass translation in the transition state. The independence of the desorption pre-exponent on N has also been observed in prior work. Handschuh *et al.* used TPD to study the desorption kinetics of ethylene glycol and polyethylene glycol oligomers from a silica surface.⁴⁹ Desorption spectra were obtained for oligomers ranging in molecular weight from 62 to 35 000 g/mole. Although the high molecular weight polyethylene glycols decomposed during heating, desorption of oligomers having molecular weights <600 g/mole desorption was observed to be both molecular and reversible and was characterized by first-order kinetics. The pre-exponential factors for desorption of the low mass polyethylene glycol oligomers were found to be independent of chain length with an average value on the order of $\nu=10^{16.3}$ s $^{-1}$. This observation further validates our observation that a single averaged pre-exponential factor may be used to model the desorption kinetics of all of the n -alkanes used in our study.

C. Desorption barriers for n -alkanes on graphite

The desorption barriers for *all* of the n -alkanes must be calculated and compared to one another in order to gain insight into the role that chain length and conformational entropy plays in determining their desorption kinetics. We

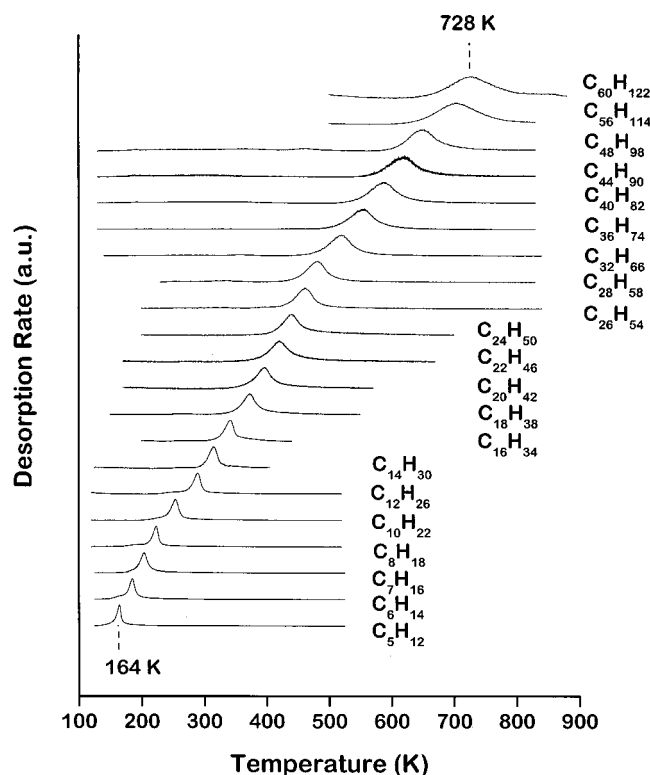


FIG. 7. TPD spectra of all *n*-alkanes studied following adsorption of approximately one monolayer on the graphite surface at 120 K. Both the desorption peak temperature and peak width increase with increasing chain length. The peak desorption temperatures of each *n*-alkane have been used to estimate their barriers to desorption, $\Delta E_{\text{des}}^{\ddagger}$. All spectra were generated using a mass spectrometer to monitor the signals at either $m/q = 57$ (C_4H_9^+) or $m/q = 71$ (C_5H_7^+) during heating. The heating rate was 2 K/s in all cases.

present below two different approaches used to obtain the desorption barriers for all of the *n*-alkanes on graphite. Section III C 1 will detail a Redhead analysis of the TPD spectra for all the *n*-alkanes to determine their desorption barriers, $\Delta E_{\text{des}}^{\ddagger}$. Section III C 2 will discuss a fitting of the TPD spectra for the *n*-alkanes to obtain both their $\Delta E_{\text{des}}^{\ddagger}$ and intermolecular interaction parameters, α .

1. $\Delta E_{\text{des}}^{\ddagger}$ obtained by Redhead analysis

$\Delta E_{\text{des}}^{\ddagger}$ of all 21 *n*-alkanes studied on graphite were determined using a Redhead analysis of the TPD spectra obtained at a constant heating rate of 2 K/s for varying initial coverages. The monolayer desorption peak temperatures of each *n*-alkane were used to evaluate their $\Delta E_{\text{des}}^{\ddagger}$. The desorption spectra of the *n*-alkanes indicated very little interaction between adsorbed molecules even at coverages approaching one monolayer. Figure 7 shows TPD spectra obtained for each of the *n*-alkanes adsorbed on graphite at an initial coverage of approximately one monolayer. This figure reveals that the *n*-alkanes desorb over a broad range of temperatures but each has a fairly narrow, well-defined desorption peak and that the peak desorption temperatures increase monotonically with chain length, *N*.

The $\Delta E_{\text{des}}^{\ddagger}$ of the *n*-alkanes from the graphite surface have been estimated using Redhead's equation⁴⁸ for first-order desorption

TABLE III. The values of $\Delta E_{\text{des}}^{\ddagger}$ for *n*-alkanes on graphite obtained by analysis of the peak desorption temperatures and by fitting of the TPD spectra. Column four lists the values of the intermolecular interaction parameter determined from fitting of the spectra to Eq. (4).

Chain length, <i>N</i>	$\Delta E_{\text{des}}^{\ddagger}$ (kJ/mole) ^a	$\Delta E_{\text{des}}^{\ddagger}$ (kJ/mole) ^b	Interaction parameter, α^b
5	65.0±2.4	60.7	-0.0003
6	73.6±2.6	69.0	-0.0001
7	81.5±2.8	78.2	0.0006
8	88.2±2.9	83.1	0.0006
10	100.9±3.2	95.6	0.0004
12	114.8±3.6	108.0	-0.0003
14	124.7±3.8	119.7	-0.0001
16	134.3±4.1	128.9	0.0012
18	146.7±4.3	142.1	0.017
20	156.2±4.6	150.5	0.014
22	166.2±4.8	163.8	0.020
24	174.2±4.9	168.8	0.019
26	182.3±5.1	177.9	0.033
28	190.7±5.4	187.0	0.043
32	205.5±5.8	202.0	0.041
36	219.6±6.0	215.3	0.041
40	232.9±6.4	228.6	0.052
44	246.2±6.6	241.1	0.046
48	256.7±6.9	253.6	0.055
56	280.5±7.5	277.7	0.060
60	289.0±7.7	289.3	0.078

^aCalculated using a Redhead analysis of variable coverage TPD data with $\beta = 2$ K/s.

^bCalculated through a least squares minimization of variable coverage TPD data.

$$\frac{\Delta E_{\text{des}}^{\ddagger}}{RT_p^2} = \frac{\nu}{\beta} \cdot \exp\left(-\frac{\Delta E_{\text{des}}^{\ddagger}}{RT_p}\right) \quad (5)$$

and a pre-exponential factor of $\nu = 10^{19.6} \text{ s}^{-1}$. Although $\Delta E_{\text{des}}^{\ddagger}$ were previously determined for several of the *n*-alkanes through a Redhead analysis of the variable heating rate TPD experiments (Sec. III B 1), those are not significantly different from $\Delta E_{\text{des}}^{\ddagger}$ calculated using the averaged pre-exponential factor of $10^{19.6} \text{ s}^{-1}$, differing by at most 7%. This study focuses on the dependence of $\Delta E_{\text{des}}^{\ddagger}$ on *N* so we rely on $\Delta E_{\text{des}}^{\ddagger}$ calculated by using the peak desorption temperatures measured for a heating rate of 2 K/s. $\Delta E_{\text{des}}^{\ddagger}$ are listed in Table III. The values of $\Delta E_{\text{des}}^{\ddagger}$ increase monotonically with the chain length, but as will be shown below the dependence on chain length is nonlinear.

2. Fitting of desorption spectra to obtain desorption barriers

In addition to using the Redhead method, $\Delta E_{\text{des}}^{\ddagger}$ for the *n*-alkanes on graphite have also been estimated by fitting the TPD spectra measured at a constant heating rate of 2 K/s to spectra simulated using Eq. (4) with varying values of the fitting parameters $\Delta E_{\text{des}}^{\ddagger}$ and α . In a procedure similar to that outlined in Sec. III B 2, the TPD spectra data obtained for each *n*-alkane at all submonolayer coverages were fit simultaneously. Since the fixed heating rate desorption spectra do not decouple $\Delta E_{\text{des}}^{\ddagger}$ and ν the value of ν has been fixed constant at $\nu = 10^{19.1} \text{ s}^{-1}$, the average value of this parameter determined by fitting of the variable heating rate TPD spectra in Sec. III B 2. Figure 8 displays the fits of the simulated

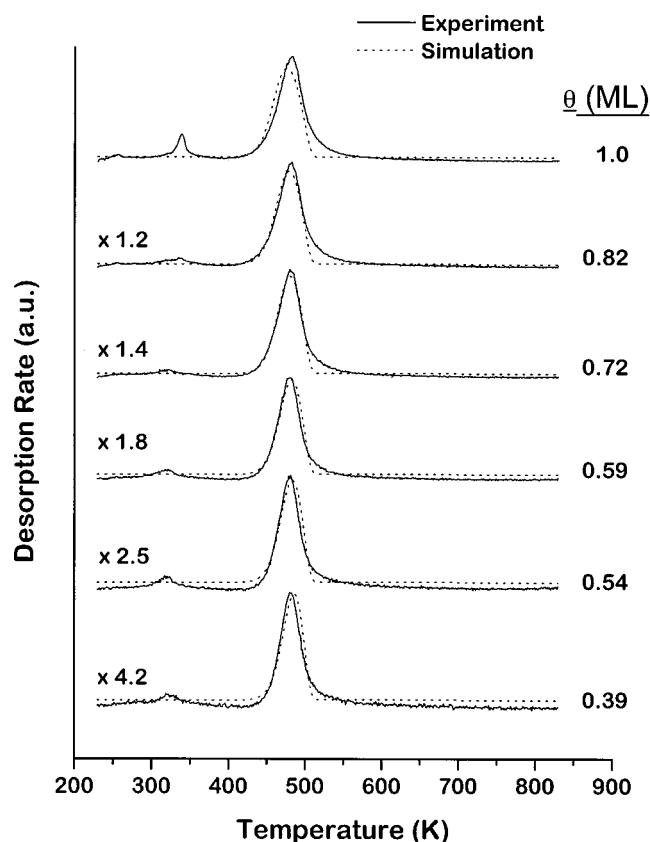


FIG. 8. Fits of simulated desorption spectra to the TPD spectra recorded for $C_{28}H_{58}$ at a constant heating rate of 2 K/s for varying initial coverages. The solid lines represent the measured TPD spectra while the dashed lines indicate the simulated spectra. The pre-exponential factor was held constant at $\nu = 10^{19.1} \text{ s}^{-1}$ during the fit. The free parameters used in the fit were found to have values of $\Delta E_{\text{des}}^{\ddagger} = 187.0 \text{ kJ/mole}$ and $\alpha = 0.043$. $\Delta E_{\text{des}}^{\ddagger}$ were observed to be of the same magnitude as those calculated via a Redhead analysis of the TPD data.

spectra to the TPD spectra of $C_{28}H_{58}$ for coverages in the range 0.39–1.0 monolayers and qualitatively illustrates the accuracy of the fits for the remaining n -alkanes. The free parameters $\Delta E_{\text{des}}^{\ddagger}$ and α of $C_{28}H_{58}$ assumed values of 187.0 kJ/mole and 0.043, respectively. More importantly, $\Delta E_{\text{des}}^{\ddagger}$ for the n -alkanes determined through both the Redhead analysis and the fitting method are of the same magnitude and vary by a maximum of $\sim 7\%$. Table III summarizes $\Delta E_{\text{des}}^{\ddagger}$ for the n -alkanes as determined by both of these methods in addition to providing the intermolecular interaction parameter, α , for each molecule. It should be pointed out that an exact comparison cannot be made between the values of $\Delta E_{\text{des}}^{\ddagger}$ determined by the two methods. Note that $\Delta E_{\text{des}}^{\ddagger}$ of the n -alkanes determined from a Redhead analysis are average values measured at the peak desorption temperature, T_p , where the coverage is roughly one-half its initial value. In contrast, $\Delta E_{\text{des}}^{\ddagger}$ determined from fitting of the TPD spectra are measured in the limit of zero coverage. The differences in the values of $\Delta E_{\text{des}}^{\ddagger}$ measured by both methods are minor because $\Delta E_{\text{des}}^{\ddagger}$ are fairly independent of coverage.

3. Chain length dependence of $\Delta E_{\text{des}}^{\ddagger}$

The $\Delta E_{\text{des}}^{\ddagger}$ for the n -alkanes on graphite have been determined using both a Redhead analysis and by fitting of

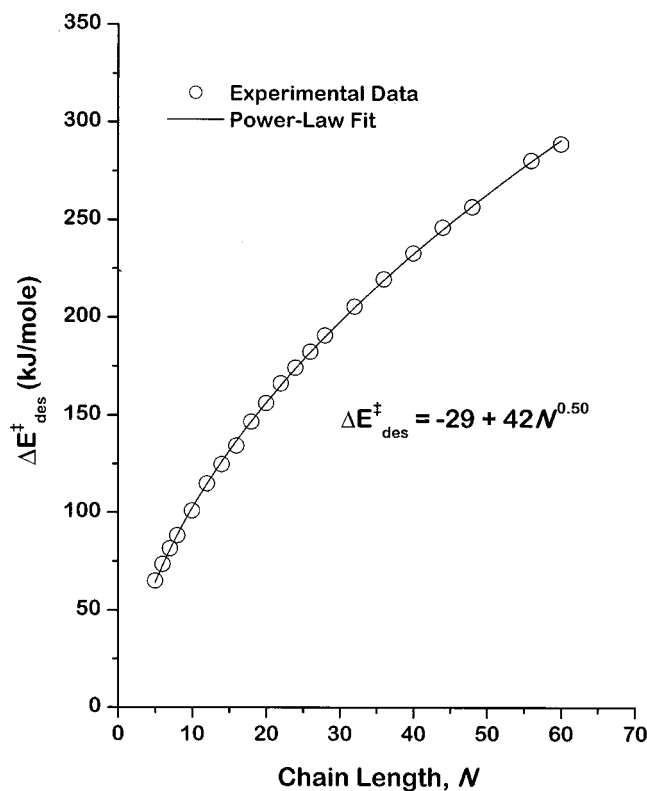


FIG. 9. Desorption barriers, $\Delta E_{\text{des}}^{\ddagger}$, of the n -alkanes from graphite as a function of chain length, N . The desorption barriers reported have been calculated using a Redhead analysis of the TPD data measured at a constant heating rate of 2 K/s. These data clearly indicate that the desorption barrier is nonlinear in the n -alkane chain length. The dashed line represents the results of fitting a power-law to the data of the form $\Delta E_{\text{des}}^{\ddagger} = a + bN^{\gamma}$, with the parameters taking on values of $a = -29 \pm 4 \text{ kJ/mole}$, $b = 42 \pm 2$ and an exponent of $\gamma = 0.50 \pm 0.01$.

TPD spectra measured using a constant heating rate of 2 K/s and varying initial coverages. Both methods yield roughly the same results for $\Delta E_{\text{des}}^{\ddagger}$ but the fitting method has the added value of providing some insight into the magnitude of the intermolecular interaction parameters. We have chosen to investigate the effects of chain length on $\Delta E_{\text{des}}^{\ddagger}$ using the data from the Redhead analysis presented in Sec. III C 1. Figure 9 illustrates $\Delta E_{\text{des}}^{\ddagger}$ of the n -alkanes on graphite as a function of the chain length, N . This figure clearly illustrates that the relationship between $\Delta E_{\text{des}}^{\ddagger}$ and N is nonlinear over the range of chain lengths explored in this work. As a first approach to the analysis of the nonlinear dependence of $\Delta E_{\text{des}}^{\ddagger}$ on chain length we have fit the data to a power law expression of the form $\Delta E_{\text{des}}^{\ddagger} = a + bN^{\gamma}$. The reason for including the offset, a , rather than using pure power law scaling ($\propto N^{\gamma}$) is that the ends of the molecules are unlikely to have the same interaction with the surface as the chain segments in the interior of the molecule. At the low end of the range of n -alkanes that we have used this will certainly be a significant contribution to $\Delta E_{\text{des}}^{\ddagger}$ and the offset, a , is a correction for that effect. The fitting parameters found for $\Delta E_{\text{des}}^{\ddagger}$ dependence on chain length are $a = -29 \pm 4 \text{ kJ/mole}$, $b = 42 \pm 2$ and the exponent is $\gamma = 0.50 \pm 0.01$. The fit to the data is shown as the solid line in Fig. 9 and reproduces the data extremely well. It is interesting to note that the extrapo-

lation of the expression for $\Delta E_{\text{des}}^{\ddagger}$ yields a value of 13 kJ/mole for $\Delta E_{\text{des}}^{\ddagger}$ of methane from graphite which is extremely close to the well-determined experimental value of 12.2 kJ/mole for the heat of adsorption of methane on graphite.^{50,51} This close comparison may be fortuitous since the extrapolated value of $\Delta E_{\text{des}}^{\ddagger} = 30$ kJ/mole for ethane does not match as closely with the experimental, although less well-determined, value of 17.2 kJ/mole for the heat of adsorption of ethane on graphite.⁵¹ Nonetheless the fit for $N=5$ to 60 reproduces the data extremely well. As a final point of comparison, a power-law fit to the values of $\Delta E_{\text{des}}^{\ddagger}(N)$ determined through simulation of the TPD spectra (Sec. III C 2) gave fitting parameters of $a = -25 \pm 5$ kJ/mole, $b = 36 \pm 3$, and $\gamma = 0.53 \pm 0.01$. This fit also reproduced the data extremely well and the values of the fitting parameters were found to be nearly identical to those determined from the power-law fit to the values of $\Delta E_{\text{des}}^{\ddagger}(N)$ found from the Redhead analysis of the TPD spectra.

In view of the fact that there are many room temperature images of the *n*-alkanes on graphite which show that these molecules lie in a straight, all-*trans* configurations on the surface, it is extremely interesting that $\Delta E_{\text{des}}^{\ddagger}$ do not scale linearly in chain length. The implication is that at the desorption temperature, configurational entropy in either the initial state or the transition state to desorption decreases the net $\Delta E_{\text{des}}^{\ddagger}$ for the longer chain oligomers. The fact that $(\Delta E_{\text{des}}^{\ddagger} - a)$ scales as $N^{1/2}$ is also intriguing. It should be noted that a true power-law representation of $\log(\Delta E_{\text{des}}^{\ddagger})$ versus $\log(N)$ yields a curve with a slope of 0.65 at $N=5$ that tends to 0.55 at $N=60$. These results suggest that as a result of configurational entropy the number of monomers interacting with the surface at the desorption temperature is of the order $N^{1/2}$ rather than N .

IV. DISCUSSION

The desorption problem described in this paper is very similar to that of a polymer interacting with a solid surface but is, of course, a case in which the polymer is of short chain length. In language commonly used to describe polymer adsorption the system described here would be one in which the polymer is desorbing from a strongly interacting surface (graphite) into a poor and infinitely dilute solvent (vacuum). Theoretical descriptions of such systems are usually framed in terms of polymer configurations involving “trains” of segments in contact with the surface, separated by “loops” of detached segments, and terminated by “tails” which are also detached from the surface. As mentioned, a fit of $\Delta E_{\text{des}}^{\ddagger}(N)$ shows that it can be described empirically with a function of the form $a + bN^{\gamma}$ where $\gamma = 0.50 \pm 0.01$. Theories have predicted that for a polymer of length N adsorbing from a melt the fraction of adsorbed segments should scale as $N^{1/2}$.^{52–54} This suggests that $\Delta E_{\text{des}}^{\ddagger}$ might also exhibit the same scaling with N under such conditions. Such theories and simulations most commonly describe equilibrium properties. Recent simulations, however, have also shown that dynamic properties such as polymer detachment rate from a surface might also scale as $N^{1/2}$. This has been observed in an experiment that measured the friction associated with the

detachment of a polymer into a melt. The detachment rate from a strongly interacting surface in this case was observed to scale as $N^{1/2}$.⁵² The system studied in this work, however, is quite different from those described or studied in the past in that we are measuring the barrier to desorption, $\Delta E_{\text{des}}^{\ddagger}$, into an infinitely dilute solution rather than a melt. The origin of the scaling behavior that we observe remains something of a mystery but is nevertheless intriguing. The remainder of this paper describes a model which captures the curvature of $\Delta E_{\text{des}}^{\ddagger}(N)$ without explicitly addressing the origin of the scaling parameter, γ .

In order to describe the dependence of $\Delta E_{\text{des}}^{\ddagger}$ on N observed in our experiments we have chosen to model the system using transition state theory as the basis for describing the desorption rate constant. Our analysis of this behavior requires a description of the mechanism by which desorption occurs and a model for the interaction energy and entropy of the chains on the surface. The desorption mechanism will be described in Sec. IV A. The interactions, energetics, and entropy of the oligomers are dependent on their configuration on the surface. These interactions are given in terms of segmental parameters such as the segment-surface interaction energy and are described in Sec. IV B. The description of the desorption mechanism and the oligomer-surface interaction are then combined in Sec. IV C to predict the observed $\Delta E_{\text{des}}^{\ddagger}(N)$ using the microscopic segment-surface interaction energies as fitting parameters.

A. Oligomer desorption mechanism

The desorption kinetics of small molecules from surfaces are measured and studied routinely using TPD spectroscopy. Desorption of small molecules from a surface is usually considered in terms of a fairly simple potential energy surface with a single reaction coordinate that describes the motion of the adsorbate from its adsorbed state into the gas phase. $\Delta E_{\text{des}}^{\ddagger}$ is the difference in the zero-point energy of the adsorbed species and the energy of a transition state that lies along the reaction coordinate leading from the adsorption well into vacuum. Although the adsorbate-surface interaction potential has many degrees of freedom in addition to the reaction coordinate for desorption, for a polyatomic adsorbate one generally thinks of these as contributing to the desorption rate constant only through the partition functions for the adsorbed species and the transition state to desorption. If the adsorbed *n*-alkanes used in this work were thought of as rigid rods and desorption were simply translation of the center-of-mass along the surface normal, then this simple description would be adequate. However, such a description of the system would tend to predict that $\Delta E_{\text{des}}^{\ddagger}$ should be linear in the chain length, N , and that is obviously not the case.

There are many STM images of long straight chain *n*-alkanes adsorbed on the surface of graphite that reveal straight all-*trans* structures at room temperature.^{16–21} At temperatures above room temperature but below the desorption temperature such images cannot be obtained because of segmental motion and disorder. This indicates that the desorption of oligomeric species such as the *n*-alkanes cannot be thought of as simple motion along a single reaction coordi-

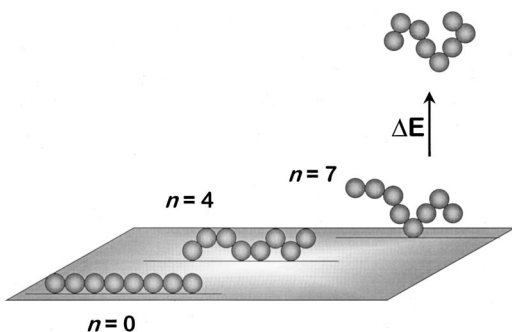


FIG. 10. Hypothetical conformations adopted by an n -alkane chain of length $N=8$ on the graphite surface. The ground state is one in which the n -alkane molecule lies in an all-*trans* conformation and has no detached segments ($n=0$). An intermediate state is depicted in which the n -alkane chain is adsorbed in a conformation with four of its eight segments detached ($n=4$). The adsorbed state that exists prior to desorption is also depicted and is one in which all-but-one of the chain segments is detached ($n=N-1=7$). The conformations adopted in each of these states are in equilibrium with one another and the relative concentrations of each are related by simple equilibrium constants.

nate. One can imagine the oligomer passing through many possible, energetically equivalent configurations on the surface as its structure approaches a number of possible and energetically equivalent transition states to desorption. In essence, there is a multiplicity of energetically equivalent pathways or reaction coordinates along which desorption might occur. This multiplicity of paths must be included within a model for the desorption process.

Consider the adsorbed oligomers as consisting of N segments each of which can be described as being in either an *attached* or a *detached* state. The segments each attach and detach from the surface reversibly and independently. The state of a particular molecule will be described by the number of detached segments, n . For example, Fig. 10 shows an oligomer of length $N=8$ in three states: fully attached ($n=0$), partially detached ($n=4$), and having all-but-one segments detached ($n=N-1=7$). The oligomer coverages in each of these states are given by θ_n and the total oligomer coverage is given by θ . The rapid and reversible attachment and detachment of individual segments means that equilibrium is established among the species in differing stages of detachment and the coverages are all related by equilibrium constants, K_n , as follows:

$$\theta_n = K_n \theta_0 = \theta_0 \cdot \exp\left(\frac{-\Delta A_n}{RT}\right)$$

The free energy differences ΔA_n are all referenced to the free energy of the fully adsorbed state which will have $A_0=0$. For an oligomer of length N the total coverage of adsorbed species, θ , can be written in terms of the coverage of species that are fully adsorbed, θ_0 :

$$\theta = \sum_{n=0}^{N-1} \theta_n = \theta_0 \cdot \sum_{n=0}^{N-1} \exp\left(\frac{-\Delta A_n}{RT}\right) = \theta_0 \cdot \Gamma.$$

The second element of the oligomer desorption mechanism is that the only species that are capable of desorbing at any instant in time are those with just one segment left attached, $n=N-1$. This desorption step is irreversible in that

once the last tether to the surface is broken and the oligomer is in vacuum it does not return to the surface. The desorption rate constant is of the form

$$k_{N-1} = \nu \cdot \exp\left(-\frac{\Delta E}{RT}\right)$$

with the barrier to this last irreversible step, ΔE , being given by the zero-point energy differences between the species with $n=N-1$ and the transition state to desorption, $\Delta E = E^\ddagger - E_{N-1}$. The pre-exponent would be given by transition state theory as

$$\nu = \left(\frac{k_B T}{h}\right) \frac{q^\ddagger}{q_{N-1}},$$

where the partition functions are for the species with $n=N-1$ detached segments, q_{N-1} , and for all degrees of freedom of the transition state other than the desorption coordinate, q^\ddagger . Finally, the rate of desorption can be expressed in terms of θ_{N-1} or, more usefully, the total coverage, θ :

$$\begin{aligned} r &= k_{N-1} \cdot \theta_{N-1} \\ &= k_{N-1} \cdot \theta_0 \cdot \exp\left(\frac{-\Delta A_{N-1}}{RT}\right) \\ &= k_{N-1} \cdot \frac{1}{\Gamma} \cdot \exp\left(\frac{-\Delta A_{N-1}}{RT}\right) \cdot \theta. \end{aligned}$$

The summation over the equilibrium constants, Γ , will always be dominated by the term with the minimum free energy, ΔA_{\min} :

$$\begin{aligned} \Gamma &= \exp\left(\frac{-\Delta A_{\min}}{RT}\right) \cdot \sum_{n=0}^{N-1} \exp\left(\frac{\Delta A_{\min} - \Delta A_n}{RT}\right) \\ &= \exp\left(\frac{-\Delta A_{\min}}{RT}\right) \cdot \Gamma'. \end{aligned} \quad (6)$$

Substitution of this expression and the expression given for the desorption rate constant into the rate equation gives an apparent first-order rate constant of

$$\begin{aligned} k_{\text{app}} &= \nu \cdot \exp\left(\frac{-\Delta E}{RT}\right) \cdot \frac{1}{\Gamma'} \cdot \exp\left(\frac{-(\Delta A_{N-1} - \Delta A_{\min})}{RT}\right) \\ &= \frac{\nu}{\Gamma'} \cdot \exp\left(\frac{S_{N-1} - S_{\min}}{R}\right) \cdot \exp\left(\frac{-(E_{N-1} - E_{\min}) - \Delta E}{RT}\right). \end{aligned}$$

The quantity Γ' , defined by Eq. (6), is a summation over the number of segments, N , of terms with values ≤ 1 . Thus for the molecules used in this work it can at most take on a value equal to the number of segments in the molecule. In reality Γ' has values ranging from 1 to ~ 10 while the rate constants for desorption range in value over ~ 35 orders of magnitude. More importantly Γ' is quite insensitive to temperature and thus the apparent rate constant yields an expression for the measured desorption barrier.

The mechanism described above gives an expression for the measured desorption barrier of an oligomer with N segments as the difference between the zero-point energies of the transition state for desorption and the species with minimum free energy:

$$\Delta E_{\text{des}}^{\ddagger}(N) = E^{\ddagger} - E_{\text{min}} = (E_{N-1} - E_{\text{min}}) + \Delta E. \quad (7)$$

At a given temperature the value of E_{min} will be determined by the number of detached segments in the species with minimum free energy, A_{min} , and must be determined on the basis of a model which gives the energy, E_n , and entropy, S_n , of the partially detached oligomers.

B. Oligomer-surface interaction model

In order to evaluate $\Delta E_{\text{des}}^{\ddagger}(N)$ within the framework of the mechanism described above and in terms of microscopic oligomer-surface interaction parameters we must propose a model that allows us to calculate the adsorption energy and the entropy of the oligomer in each of its possible configurations on the surface. To begin we define the number of segments in the *n*-alkanes as the number of *bonds* rather than the number of methylene units or carbon atoms. In other words the species used in this work have $N-1=4$ to 59 segments, where N is the number of carbon atoms. Detachment of a segment then is the detachment of a bond from the surface. The reason for using this model rather than considering the number of segments to be the number of carbon atoms will become apparent when calculating the number of conformations available to a species with n detached bonds.

The reference energy state of the adsorbed alkanes will be those molecules with no detached segments, $E_0=0$. This is the state observed for a number of long *n*-alkanes adsorbed on graphite in a straight all-*trans* chain at room temperature.¹⁶⁻²¹ The energy of a species with n of its $N-1$ bonds detached from the surface is given by the expression

$$E_n^N = n \cdot E^{bs}. \quad (8)$$

In other words, the energy is simply proportional to the number of desorbed segments with the bond-surface interaction energy, E^{bs} , being an unknown parameter.

The configurational entropy of the partially detached oligomer is given by the configurational partition function, q_n^N , through the Boltzmann equation. For an oligomer with n of its $N-1$ bonds detached from the surface the configurational partition function is

$$q_n^N = \frac{(N-1)!}{n!(N-1-n)!} \cdot 3^n.$$

The first term simply accounts for the number of ways to detach n of $N-1$ bonds from the surface. The second term is particular to the *n*-alkanes and accounts for the three rotational conformations (*trans*, *+gauche*, and *-gauche*) that can be adopted by each detached C-C bond. This assumes that those bonds that are attached to the surface are restricted to one configuration, presumably the *trans* configuration observed in scanning tunneling micrographs. Finally, the expression for the entropy, S_n^N of a species in a configuration with n of $N-1$ bonds detached is given by

$$S_n^N = R \cdot \left[\ln \left(\frac{(N-1)!}{n!(N-1-n)!} \right) + n \cdot \ln 3 \right].$$

C. Oligomer desorption kinetics

Using the model defined above for the desorption mechanism and the oligomer-surface interaction we have compared the predicted and experimental values of the desorption barriers in order to determine the ability of the model to predict the nonlinearity of $\Delta E_{\text{des}}^{\ddagger}(N)$. For each oligomer we determine the number of detached bonds, n_{min} , which minimizes the free energy

$$A_n^N = E_n^N - T_p^N S_n^N.$$

Note that the temperatures used are the peak desorption temperatures, T_p , which are the temperatures at which the desorption barriers were measured. Also note that the value of E_n^N depends on the undetermined parameter, E^{bs} . Using the value of n_{min} which minimizes the A_n^N one can predict the value of $\Delta E_{\text{des}}^{\ddagger}(N)$ using Eq. (7). Note also that the expression for $\Delta E_{\text{des}}^{\ddagger}(N)$ includes the second free parameter in the model which is ΔE , the desorption barrier for the last segment attached to the surface (Fig. 10). To be clear it should be mentioned here that our predictions of $\Delta E_{\text{des}}^{\ddagger}(N)$ have been made in all cases by equating the number of segments to the number of bonds rather than the number of carbon atoms, N . This implies that the desorption barrier would now be given by a modified version of Eq. (7):

$$\Delta E_{\text{des}}^{\ddagger}(N) = (E_{N-2} - E_{\text{min}}) + \Delta E, \quad (7')$$

where the subscripts refer to the number of detached bonds. Finally, this problem can be solved using the two free parameters E^{bs} and ΔE to fit the predicted values of $\Delta E_{\text{des}}^{\ddagger}(N)$ to the 21 experimentally measured values of $\Delta E_{\text{des}}^{\ddagger}(N)$. Figure 11 illustrates a comparison between the experimental values of $\Delta E_{\text{des}}^{\ddagger}(N)$ and the theoretical fit drawn with the dashed line. There is an almost exact agreement between the two and this simple model completely reproduces the nonlinear dependence of $\Delta E_{\text{des}}^{\ddagger}$ on chain length. Figure 12 plots the values of n_{min} for each *n*-alkane oligomer at its desorption temperature. Note that the number of detached segments at the desorption temperature increases with chain length and that for the long chains the minimum free energy configuration has a significant fraction of detached segments at the desorption temperature. In looking at this plot it is important to realize that $\Delta E_{\text{des}}^{\ddagger}(N)$ scales as $N-2-n_{\text{min}}$.

It is important to consider the values of the free parameters predicted by the fit of the theoretical values of $\Delta E_{\text{des}}^{\ddagger}(N)$ to our experimental data and to decide whether these are physically reasonable. First, the predicted value of the bond-surface interaction energy is $E^{bs} = 8.0$ kJ/mole/bond. It is important to realize that physically this parameter may include both interaction with the graphite surface and the interactions between adsorbed chains. Previous measurements of the interaction of much shorter alcohols and alkanes with metals such as Ag,²⁴ Cu,^{42,43} and Au²⁵ have yielded values in the range 5–6 kJ/mole/CH₂ group. A recent study by Bishop *et al.* has reported segment-surface interaction energies of ~ 8 kJ/mole/CH₂ group for *n*-alkanes ($N=6$ to 10) adsorbed on Pt(111).⁵⁵ The predicted value of ΔE must also be explored to ensure that its magnitude is physically reasonable. As defined in Sec. IV A, ΔE is the energy needed to

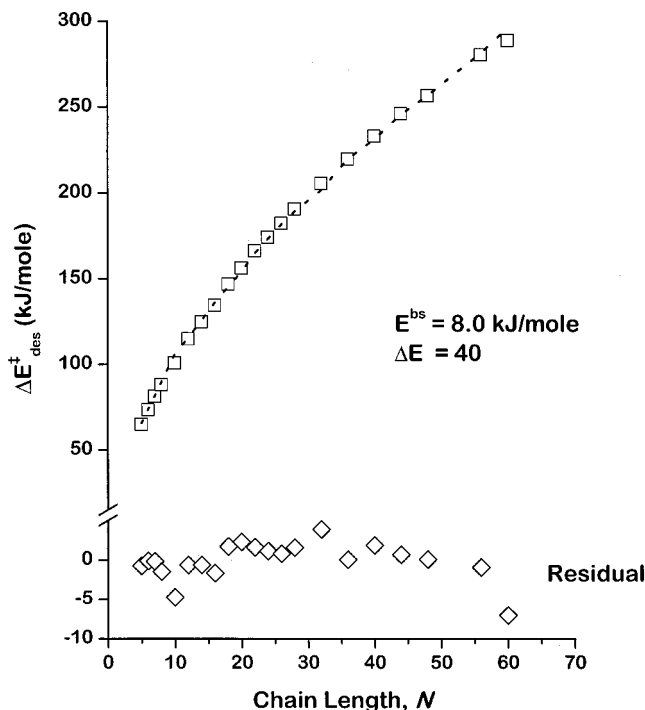


FIG. 11. Comparison of the experimentally determined values of $\Delta E_{\text{des}}^{\ddagger}$ with those predicted by the theory described in this paper. The results of the theoretical fits are given by the dashed line through the data. The residual errors or difference between the theory and experiments are shown at the bottom.

irreversibly detach the last adsorbed bond from the surface. At first glance the predicted value of $\Delta E = 40$ kJ/mole may seem high since one would expect it to be of similar magnitude to E^{bs} . The significance of ΔE , however, is more complicated. As used in the expression for $\Delta E_{\text{des}}^{\ddagger}(N)$ in Eq. (7') it represents an offset to the values of $(E_{N-2} - E_{\text{min}})$. It is important to keep in mind that the oligomers that we have used are far from being infinite polymers and that end effects are likely to be observable. In essence ΔE , the offset to the values of $\Delta E_{\text{des}}^{\ddagger}(N)$, also accounts for the difference between the bond-surface interaction at either end of the molecule and the bond-surface interaction in the middle, E^{bs} . In this sense the value of ΔE can be thought of as having three contributions. One contribution is from the interaction of the last remaining bond with the graphite surface expected to be on the order of E^{bs} . The remaining two contributions would be equated to the energy needed over and above that of E^{bs} to desorb each of the two terminal endgroup bonds. In other words, the value of ΔE can be thought of as arising from two endgroup contributions of roughly 16 kJ/mole each and an energetic interaction of the last remaining bond on the surface of ~ 8 kJ/mole. Each of these contributions is of a plausible magnitude.

One might imagine that interactions between detached segments might favor configurations with many detached segments and thus contribute to the nonlinearity of $\Delta E_{\text{des}}^{\ddagger}(N)$. This possibility was considered by including a mean-field term in the expression for the energy of species with n detached segments:

$$E_n^N = n \cdot E^{bs} + \frac{1}{2}n(n-1)E^{bb}. \quad (8')$$

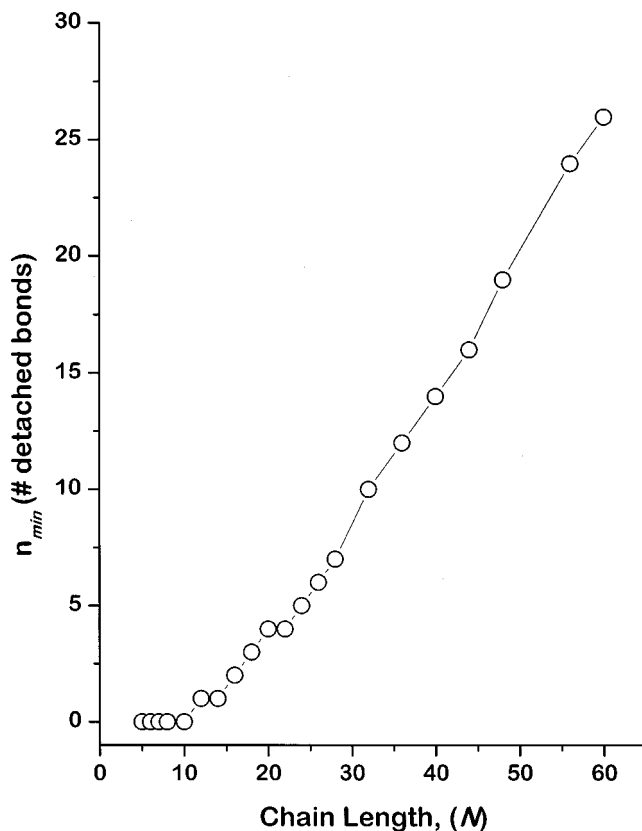


FIG. 12. The number of detached bonds, n_{min} , at desorption for the n -alkane oligomers used in this study. The values of n_{min} are the values which have minimized the free energy of the adsorbed state at the desorption temperature, T_p . The value of n_{min} clearly increases with increasing chain length although in a nonlinear fashion. The desorption barrier is given as $\Delta E_{\text{des}}^{\ddagger} = E_{N-2} - E_{\text{min}} + \Delta E$ and therefore also increases with chain length but with a nonlinear dependence on N .

The term E^{bb} is now an additional free parameter in the model and represents the bond-bond interactions among desorbed segments of a molecule. The fit of theoretical to experimental values of $\Delta E_{\text{des}}^{\ddagger}(N)$ is, of course, improved by this addition since the model now contains three free parameters. However, the improvement is minor and the magnitude of the mean field parameter which represents the interaction between detached bonds is very low, $E^{bb} = 0.007$ kJ/mole/bond². Interactions between detached bonds account for less than 1% of $\Delta E_{\text{des}}^{\ddagger}(N)$, even in the longest n -alkane, and do not contribute at all to $\Delta E_{\text{des}}^{\ddagger}(N)$ of the short n -alkanes. The primary observations of this fitting are that the model described in Secs. IV A and IV B clearly reproduces the nonlinear chain length dependence of $\Delta E_{\text{des}}^{\ddagger}(N)$ and that this nonlinear behavior is primarily due to conformational entropy effects.

Finally, it is worth mentioning the origin of the relatively high value of $10^{19.6} \text{ s}^{-1}$ observed for the desorption pre-exponent of the alkanes on graphite. In this problem the apparent or observed pre-exponent is given by

$$\nu_{\text{app}} = \frac{1}{\Gamma'} \cdot \left(\frac{k_B T}{h} \right) \frac{q_{\ddagger}}{q_{N-1}} \cdot \exp\left(\frac{S_{N-1} - S_{\text{min}}}{R} \right).$$

As mentioned the value of Γ' does not contribute more than a factor of 10. The partition functions are those for the spe-

cies with all-but-one bond detached, q_{N-1} , and for the transition state to desorption, q_{\ddagger} . The final term is due to the difference in configurational entropy of the species with minimum free energy and the species with all-but-one bond detached. This can be quite significant and for the range of chain lengths studied in this work it contributes on average a factor of $10^{3.4}$ to the apparent desorption pre-exponent. Thus, it is apparent that one should observe relatively high values of the desorption pre-exponent for oligomer desorption from surfaces.

V. CONCLUSIONS

The desorption kinetics of oligomers from surfaces has been shown to be influenced by chain length. The measured desorption energies are clearly nonlinear in chain length. This is not surprising given the multiplicity of desorption paths that can be taken by molecules such as oligomers that have many different energetically equivalent conformations. We have proposed a model in which adsorbed *n*-alkanes can adopt numerous configurations in which some segments are detached and those that are detached adopt a mixture of *gauche*, *+trans*, and *-trans* configurations. This model successfully predicts the nonlinear dependence of $\Delta E_{\text{des}}^{\ddagger}(N)$ on the oligomer chain length, N .

ACKNOWLEDGMENTS

Support from the NSF (CMS-9900647) and from the National Storage Industries Consortium (NSIC) is acknowledged for this work. The development of the high molecular weight doser was supported by the AFOSR (F49620-96-1-0253).

- ¹J.-J. Lee and G. G. Fuller, *J. Colloid Interface Sci.* **103**, 569 (1985).
- ²J. N. Israelachvili, *Intermolecular and Surface Forces* (Academic, New York, 1985).
- ³J. N. Israelachvili, P. M. McGuiggan, and A. M. Homola, *Science* **240**, 189 (1988).
- ⁴F. Heslot, N. Frayasse, and A. M. Cazabat, *Nature (London)* **338**, 640 (1989).
- ⁵S. Granick, *Science* **253**, 1374 (1991).
- ⁶A. L. Demirel and S. Granick, *Phys. Rev. Lett.* **77**, 2261 (1996).
- ⁷D. J. Diestler, M. Schoen, and J. H. Cushman, *Science* **262**, 545 (1993).
- ⁸B. G. Min, J. W. Choi, H. R. Brown, D. Y. Yoon, T. M. O'Connor, and M. S. Jhon, *Tribol. Lett.* **1**, 225 (1995).
- ⁹T. E. Karis and G. W. Tyndall, *J. Non-Newtonian Fluid Mech.* **82**, 287 (1999).
- ¹⁰J. E. Curry and J. H. Cushman, *Tribol. Lett.* **4**, 129 (1998).
- ¹¹G. W. Tyndall, T. E. Karis, and M. S. Jhon, *IEEE Trans. Magn.* (in press).
- ¹²G. J. Fleer, M. A. Cohen Stuart, J. M. H. M. Scheutjens, T. Cosgrove, and B. Vincent, *Polymers at Interfaces* (Chapman and Hall, New York, 1993).
- ¹³M. Kawaguchi and A. Takahashi, *Adv. Colloid Interface Sci.* **37**, 219 (1992).
- ¹⁴P.-G. de Gennes, *Adv. Colloid Interface Sci.* **27**, 189 (1992).

- ¹⁵G. H. Findenegg and M. Liphard, *Carbon* **25**, 119 (1987).
- ¹⁶G. C. McGonigal, R. H. Bernhardt, and D. J. Thomson, *Appl. Phys. Lett.* **57**, 28 (1990).
- ¹⁷G. C. McGonigal, R. H. Bernhardt, Y. H. Yeo, and D. J. Thomson, *J. Vac. Sci. Technol. B* **9**, 1107 (1991).
- ¹⁸J. P. Rabe and S. Buchholz, *Science* **253**, 424 (1991).
- ¹⁹J. P. Rabe and S. Buchholz, *Makromol. Chem., Macromol. Symp.* **50**, 261 (1991).
- ²⁰J. P. Rabe and S. Buchholz, *Phys. Rev. Lett.* **66**, 2096 (1991).
- ²¹S. Buchholz and J. P. Rabe, *Angew. Chem.* **104**, 188 (1992).
- ²²A. J. Groszek, *Nature (London)* **196**, 531 (1962).
- ²³R. Zhang and A. J. Gellman, *J. Phys. Chem.* **95**, 7433 (1991).
- ²⁴B. Millot, A. Methivier, and H. Jobic, *J. Phys. Chem. B* **102**, 3210 (1998).
- ²⁵S. M. Wetterer, D. J. Lavrich, T. Cummings, S. L. Bernasek, and G. Scoles, *J. Phys. Chem. B* **102**, 9266 (1998).
- ²⁶L. Askadskaya and J. P. Rabe, *Phys. Rev. Lett.* **69**, 1395 (1992).
- ²⁷J.-P. Bucher, H. Roeder, and K. Kern, *Surf. Sci.* **289**, 370 (1993).
- ²⁸F. Y. Hansen, K. W. Herwig, B. Matthies, and H. Taub, *Phys. Rev. Lett.* **83**, 2362 (1999).
- ²⁹B. J. Haupt, J. Ennis, and E. M. Sevick, *Langmuir* **15**, 3886 (1999).
- ³⁰Y. Wang, R. Rajagopalan, and W. L. Mattice, *Phys. Rev. Lett.* **74**, 2503 (1995).
- ³¹P. Sjövall and B. Kasemo, *J. Chem. Phys.* **98**, 5932 (1993).
- ³²M. J. Nowakowski, J. M. Vohs, and D. A. Bonnell, *J. Am. Ceram. Soc.* **76**, 279 (1993).
- ³³J. N. Dickson and T. E. Daubert, *Ind. Eng. Chem. Res.* **27**, 523 (1988).
- ³⁴D. L. Morgan and R. Kobayashi, *Fluid Phase Equilib.* **97**, 211 (1994).
- ³⁵C. Vega and A. L. Rodríguez, *J. Chem. Phys.* **105**, 4223 (1996).
- ³⁶L. Reich and S. S. Stivala, *Elements of Polymer Degradation* (McGraw-Hill, New York, 1971).
- ³⁷V. Piacente, T. Pompili, P. Scardala, and D. Ferro, *J. Chem. Thermodyn.* **23**, 379 (1991).
- ³⁸M. F. Grenier-Loustalot, M. Potin-Gautier, and P. Grenier, *Anal. Lett.* **14**, 1335 (1981).
- ³⁹R. D. Chirico, A. Nguyen, W. V. Steele, and M. M. Strube, *J. Chem. Eng. Data* **34**, 149 (1989).
- ⁴⁰K. Ruzicka and V. Majer, *J. Phys. Chem. Ref. Data* **23**, 1 (1994).
- ⁴¹V. Piacente, D. Fontana, and P. Scardala, *J. Chem. Eng. Data* **39**, 231 (1994).
- ⁴²A. V. Teplyakov, A. B. Gurevich, M. X. Yang, B. E. Bent, and J. G. Chen, *Surf. Sci.* **396**, 340 (1998).
- ⁴³B. A. Sexton and A. E. Hughes, *Surf. Sci.* **140**, 227 (1984).
- ⁴⁴V. P. Zhdanov, *Surf. Sci. Rep.* **12**, 183 (1991).
- ⁴⁵A. K. Ott, S. M. Casey, and S. R. Leone, *Surf. Sci.* **405**, 228 (1998).
- ⁴⁶M. C. Flowers, B. H. Jonathan, A. Morris, and S. Wright, *Surf. Sci.* **351**, 87 (1996).
- ⁴⁷B. Bourguignon, R. V. Smilgys, and S. R. Leone, *Surf. Sci.* **204**, 473 (1988).
- ⁴⁸P. A. Redhead, *Vacuum* **12**, 203 (1962).
- ⁴⁹M. Handschuh, S. Nettesheim, and R. Zenobi, *J. Chem. Phys.* **107**, 2603 (1997).
- ⁵⁰G. Vidali, G. Ihm, H.-Y. Kim, and M. W. Cole, *Surf. Sci. Rep.* **12**, 133 (1991).
- ⁵¹N. N. Avgul and A. V. Kiselev, *Chemistry and Physics of Carbon, Volume 6*, edited by P. L. Walker (Dekker, New York, 1970).
- ⁵²X. Zheng, B. B. Sauer, J. G. Van Alsten, S. A. Schwarz, M. H. Rafailovich, J. Sokolov, and M. Rubinstein, *Phys. Rev. Lett.* **74**, 407 (1995).
- ⁵³I. A. Bitsanis and G. ten Brinke, *J. Chem. Phys.* **99**, 3100 (1993).
- ⁵⁴Y. Wang and R. Rajagopalan, *J. Chem. Phys.* **105**, 696 (1996).
- ⁵⁵A. R. Bishop, G. S. Girolami, and R. G. Nuzzo, *J. Phys. Chem. B* **104**, 754 (2000).